11706 *J. Am. Chem. Soc.* **1998,** *120,* 11706−11709

Transition Metal Complex-Doped Hydroxyapatite Layers on Porous Silicon

Xin Li,[†] Jeffery L. Coffer,*,[†] Yandong Chen,[‡] Russell F. Pinizzotto,[‡] Jon Newey,[§] and Leigh T. Canham[§]

Contribution from the Department of Chemistry, Texas Christian University, Fort Worth, Texas, 76129, Materials Science Department, University of North Texas, Denton, Texas 76203, and DRA Malvern, St. Andrews Road, Malvern, Worcestershire WR14 3PS, U.K.

Received July 6, 1998

Abstract: In this work, the encapsulation of the transition metal complexes *cis*-$Pt(NH_3)_2Cl_2$, $Ru(bpy)_3^{2+}$, and $Ru(phen)_3^{2+}$ within layers of hydroxyapatite on a porous Si/Si substrate are described. These specific complexes were selected as a consequence of their biological activity (*cis*-$Pt(NH_3)_2Cl_2$) or polynucleotide binding ability ($Ru(bpy)_3^{2+}$ and $Ru(phen)_3^{2+}$). The complex-doped hydroxyapatite/porous Si/Si materials have been characterized by scanning electron microscopy, energy-dispersive X-ray spectroscopy, secondary ion mass spectrometry, and photoluminescence spectroscopy. It is possible to exercise some control of the release of a given complex into the surrounding medium through thermal heating of the complex-doped hydroxyapatite/porous Si/Si structure.

Introduction

The observation of efficient visible light emission from thin porous films etched from single-crystal silicon (porous silicon) in 1990[1] has stimulated extensive multidisciplinary interest in this material, much of it from the perspective of the fundamental mechanism of light emission as well as the fabrication of porous Si-based optoelectronic components.[2] The utility of this matrix expanded in 1995 when it was demonstrated that layers of hydroxyapatite could be grown onto the porous Si surface, thereby rendering it biocompatible.[3] In principle, the incorporation of selected transition metal complexes into a hydroxyapatite/porous Si/Si framework could produce a hybrid material with the transition metal "dopant" complex rendering molecular recognition or biological activity to the system. While a large number of appealing candidates exist, we describe in this paper initial studies regarding the encapsulation of transition metal complexes such as *cis*-$Pt(NH_3)_2Cl_2$ (*cis*-platin or *cis*-DDP), $Ru(bpy)_3^{2+}$, and $Ru(phen)_3^{2+}$ within layers of hydroxyapatite on a porous Si/Si substrate. These complexes are of pragmatic interest due to their biological activity (anticancer—*cis*-$Pt(NH_3)_2Cl_2$)[4] or ability to bind polynucleotides ($Ru(bpy)_3^{2+}$ and $Ru(phen)_3^{2+}$).[5] In this context, one could visualize the construction of an electrically responsive biocompatible Si device capable of localized drug delivery for the treatment of bone cancer, for example. We demonstrate that, through thermal heating of the complex-doped hydroxyapatite/porous Si/Si structure, some control of the interaction of these dopants with the surrounding medium is possible. These materials have been characterized using scanning electron microscopy (SEM), X-ray energy-dispersive spectroscopy (XEDS), secondary ion mass spectrometry (SIMS), and photoluminescence (PL) spectroscopy.

Experimental Section

Sample Preparation. The fabrication process for doped hydroxyapatite/porous Si/Si structure(s) requires two distinct steps: (1) anodic etching of single-crystal Si to produce a 4 μm thick film of porous Si on the Si wafer, followed by (2) cathodic bias-induced nucleation of hydroxyapatite layers onto the porous Si layer in the presence of a dilute solution of the desired transition metal complex. The porous Si layer is prepared by anodization of low resistivity Sb-doped n-type ⟨100⟩ Si (0.008−0.02 Ω cm) for 5 min in a mixture of 48% HF/ethanol (1:1) at a current density of ~100 mA/cm². The porous Si samples were rinsed with acetone or ethanol immediately after removal from the etching solution and then dried in air for ~1 h before the deposition of complex-doped apatite. For the second step, the established acceleration of hydroxyapatite nucleation on porous Si surfaces[3b] from a mixture of ions known as simulated body fluid (SBF)[6] under cathodic bias was employed; the term SBF arises from the fact that the concentrations of ions present in SBF are nearly equal to those of human blood plasma. Each complex (1 mM)/SBF solution was prepared by dissolving the desired complex ($Ru(bpy)_3Cl_2$, $Ru(phen)_3Cl_2$, or *cis*-$Pt(NH_3)_2Cl_2$) into SBF, and the solution was used as an electrolyte. Typically, 20 mL of a given complex/SBF solution was transferred into a 100 mL glass beaker. The porous Si segment (~1.5 × ~0.5 cm) was mounted vertically in the beaker with only the porous area exposed to the electrolyte. Platinum foil was used as the counter electrode. The deposition of the complex-doped apatite layer on porous Si was achieved by applying cathodic bias to the porous Si wafer with

---

* To whom correspondence should be addressed. E-mail: j.coffer@tcu.edu.

[†] Texas Christian University.

[‡] University of North Texas.

[§] DRA Malvern.

(1) Canham, L. T. *Appl. Phys. Lett.* **1990**, *57*, 1046.

(2) For an extensive compilation of fundamental and applied research concerning porous silicon, see *Properties of Porous Silicon*, Leigh Canham, Ed., EMIS Datareviews Series, INSPEC/IEE Press (UK), 1997.

(3) (a) Canham, L. T. *Adv. Mater.* **1995**, *7*, 1033. (b) Canham, L. T.; Newey, J. P.; Reeves, C. L.; Houlton, M. R.; Loni, A.; Simons, A. J.; Cox, T. I. *Adv. Mater.* **1996**, *8*, 847. (c) Canham, L. T.; Newey, J. P.; Reeves, C. L.; King, D. O.; Branfield, P. J.; Crabb, J. G.; Ward, M. C. L. *Adv. Mater.* **1996**, *8*, 850.

(4) (a) Pratt, W.; Ruddon, R.; Ensminger, W.; Maybaum, J.; *The Anticancer Drugs*, New York: Oxford Press: 2nd ed., 1994; pp 133. (b) Pinto, A. and Lippard, S. J. *Biochim. Biophys. Acta*, **1985**, *780*, 167.

(5) Barton, J. K. *Science*, **1986**, *233*, 727.

(6) SBF was prepared from a literature procedure[3] by mixing 1.37 M NaCl, 0.03 M KCl, 0.042 M $NaHCO_3$, 0.01 M K_2HPO_4, 0.015 M $MgCl_2$, 0.025 M $CaCl_2$, and 0.005 M Na_2SO_4 solutions into a buffer of tris-hydroxymethyl-aminomethane and HCl with a final pH of 7.30 (± 0.05).

10.1021/ja9823666 CCC: $15.00

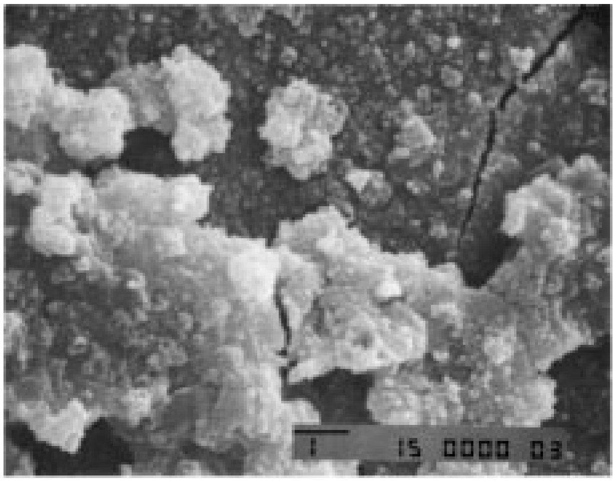

Figure 1. Plan view SEM image of a *cis*-Pt$(NH_3)_2Cl_2$-doped hydroxyapatite layer on porous Si. Scale bar shown is 1 micrometer.

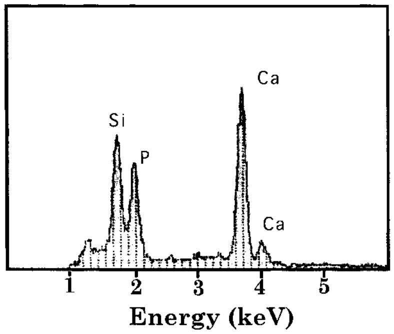

Figure 2. X-ray energy dispersive X-ray spectroscopy (XEDS) measurements indicating the presence of calcium, phosphorus, and silicon in a *cis*-Pt$(NH_3)_2Cl_2$-doped hydroxyapatite/porous Si/Si sample.

a current density of ∼1 mA/cm^2 for 3 h. The samples were rinsed with distilled, deionized (DI) water and air-dried before further characterization. It should be noted that control experiments have determined that the apatite deposition process irreversibly eliminates any visible luminescence emanating from the underlying porous Si substrate.

Instrumentation. Steady-state PL measurements were recorded using a Spex Fluorolog-2 with a 0.22-m double emission spectrometer; an excitation wavelength of 375 nm was used for the Ru complexes. Fluorescence microscopic measurements were recorded by a Nikon Optiphot-2 microscope equipped with a high-resolution Sony CCD camera. Scanning electron microscopy (SEM) was performed using a JEOL T 300 operating at 20 kV. X-ray energy-dispersive spectroscopy was measured using a Tracor-Northern TN5500 system. Secondary ion mass spectrometric (SIMS) measurements were conducted on a Cameca 4F system. Samples were sputtered using an O_2^+ ion beam at an energy of 8 keV, rastered over an area of approximately 175 μm^2.

Results and Discussion

A plan view SEM image of a *cis*-Pt$(NH_3)_2Cl_2$-doped hydroxyapatite layer on porous Si prepared by the above procedure is shown in Figure 1. The morphology of this surface is best described as an agglomeration of individual nodules whose average domain size is on the order of ∼10^2 nm. Such structures are similar to those previously observed for hydroxyapatite layers on porous Si.[3] Energy-dispersive X-ray measurements (XEDS) of these domains confirm the presence of calcium and phosphorus (as well as silicon), consistent with the formation of a calcium phosphate phase (Figure 2). However, the concentration of the platinum complex is apparently too low to detect by XEDS; therefore SIMS was used to confirm the presence of the *cis*-Pt$(NH_3)_2Cl_2$ within the apatite layers (Figure 3). With depth profiling, it is seen that the calcium signal extends up to 18 μm deep into the sample, at which point bulk Si is reached. Pt was also monitored and found to be present in the apatite/porous Si layers in the correct isotopic abundance (^{194}Pt, 32.8%; ^{196}Pt, 25.4%; ^{198}Pt, 7.2%). As anticipated, chlorine was also dectected and found to follow the same profile as Pt.

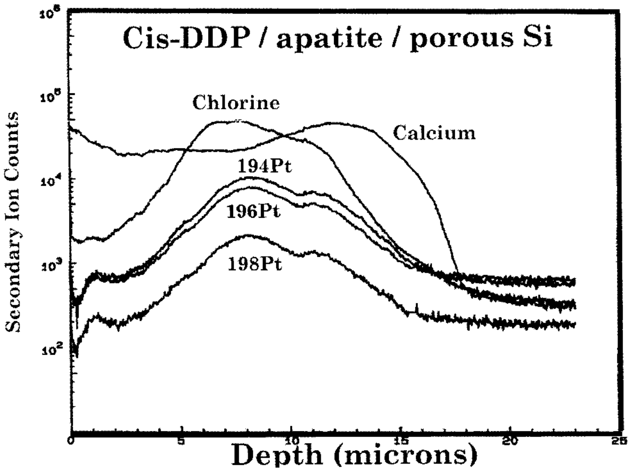

Figure 3. SIMS depth profile for *cis*-Pt$(NH_3)_2Cl_2$ (*cis*-DDP)-doped hydroxyapatite layer on porous Si, tracking the relative concentrations of chlorine, calcium, and platinum.

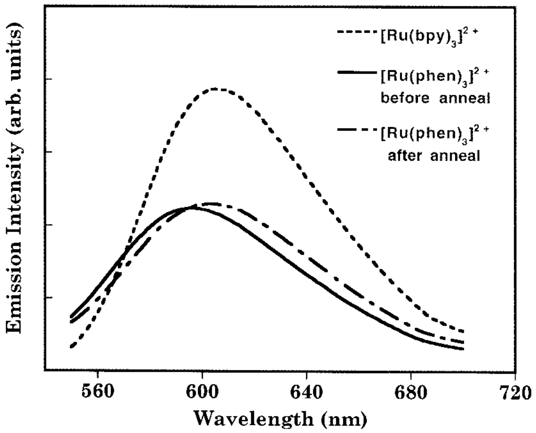

Figure 4. Room-temperature photoluminescence spectra of Ru$(bpy)_3^{2+}$ and Ru$(phen)_3^{2+}$-doped hydroxyapatite/porous Si/Si samples recorded in air at room temperature. The effect of heating the Ru$(phen)_3^{2+}$-doped hydroxyapatite/porous Si sample for 80 min at 130 °C is shown as a dashed−dot curve. The excitation wavelength used for all samples was 375 nm.

For hydroxyapatite/porous Si/Si samples doped with intrinsically fluorescent Ru$(bpy)_3^{2+}$ and Ru$(phen)_3^{2+}$, photoluminescence spectroscopy and fluorescence microscopy provide probes of incorporation of the transition metal complex within the hydroxyapatite layer (Figure 4). For these samples, the characteristic orange emission of each complex with a maximum near 600 nm is observed. Fluorescence microscopy of a Ru(phen)$_3^{2+}$ -doped hydroxyapatite/porous Si/Si sample (Supporting Information) illustrates the relatively bright orange emission emanating from apparent apatite domains (as observed by SEM analyses) on the surface. Such observations are consistent with the luminescent complex being trapped within the calcium phosphate domains. It should be noted that SIMS analyses of the Ru$(bpy)_3^{2+}$- and Ru$(phen)_3^{2+}$-doped hydroxyapatite/porous Si/Si samples are impractical because of the interference of molecular ions with larger abundances (arising from combinations of Si and O) having the same masses as the ruthenium isotopes.

While these transition metal complexes are located within the hydroxyapatite layers of the material, some portion of a given complex can diffuse out from this matrix into the surrounding medium upon solvent exposure. This behavior has important implications as to the controlled delivery of a "dopant" species from this material in future applications; thus we have been investigating the effect of thermal heating of the doped hydroxyapatite/porous Si/Si framework on the ability of the Ru complexes to diffuse into an aqueous environment. A modest temperature (130 °C) is selected, one that can alter complex/apatite interactions (through adsorbed water and surface hydroxyl groups) without degrading the complex. This heating process does not significantly alter the emission intensity of a given Ru complex but does red-shift the emission maximum slightly to longer wavelengths (~10 nm; see Figure 4). Such shifts are suggestive of minor perturbations of the secondary coordination sphere of the complex. It is also interesting to note that this temperature is also compatible with existing sterilization treatments.

One can analyze the impact of heating the doped hydroxyapatite/porous Si/Si matrix on diffusion rate from two different (and complementary) perspectives: (1) examination of the diminution of Ru complex emission intensity originating from the solid hydroxyapatite matrix as a function of time and (2) tracking the time-dependent increases in absorption and/or emission of the analyte solution as the Ru complex diffuses out from the hydroxyapatite. For the case of (1), we have compared the behavior of an as-prepared $Ru(phen)_3^{2+}$-doped hydroxyapatite/porous Si/Si matrix with that of a comparable sample that was heated in air at 130 °C for either 40 or 80 min. In these cases, the rate of decrease of Ru complex emission intensity is found to follow first-order kinetics (Supporting Figure 2) and extending the duration of the anneal has a measurable effect on slowing the rate of diminution (k_{obs} of the as-prepared sample ~ 0.005 min^{-1}; k_{obs} of the 40 min annealed sample ~ 0.001 min^{-1}; k_{obs} of the 80 min annealed sample is essentially zero). However, in these fluorescence measurements, complications can arise from the fact that as the concentration of $Ru(phen)_3^{2+}$ in the apatite is reduced upon out-diffusion, the extent of quenching due to intercomplex energy transfer is reduced and hence the emission intensity can increase. In an annealed sample, where the complex is relatively more strongly bound to the apatite, these two competing phenomena could offset each other.

To quantitatively address how much Ru complex is diffusing from the hydroxyapatite into an aqueous supernatant, experiments along the lines of (2) must be performed. Interestingly, for the sample heated at 130 °C for 80 min, initial exposure to water results in the rapid, linear increase in the 446 nm absorption maximum of the $Ru(phen)_3^{2+}$ complex in the aqueous solution, corresponding to an initial diffusion rate of 1×10^{-7} M min^{-1}; an equilibrium concentration of 10 mM can be reached (Figure 5). Replacement of this Ru complex solution with fresh DI water results in a second release of the complex at a diminished rate of 1×10^{-8} M min^{-1} into the surroundings and a corrsespondingly lower equilibrium concentration (~100 nM). This process can be repeated with an incremental diminution of the rate of complex dissolution into the solvent; such experiments suggest that the amount of complex delivered to the surroundings can be "tailored" by thermal annealing of the doped hydroxyapatite/porous Si/Si sample.

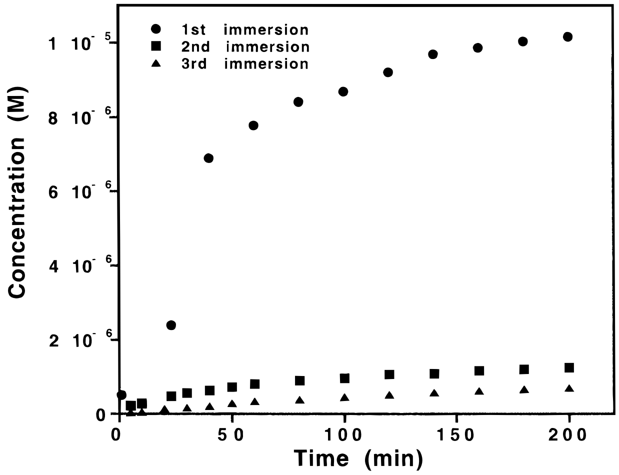

Figure 5. Changes in $Ru(phen)_3^{2+}$ concentration as a function of time for an aqueous supernatant in contact with a $Ru(phen)_3^{2+}$-doped hydroxyapatite/porous Si/Si sample. Solution concentrations are determined spectrophotometrically by monitoring changes in the absorbance at 446 nm and employing an ϵ value of 20,000 M^{-1} cm^{-1}. After each immersion experiment, the supernatant is removed from the sample compartment, fresh DI water is introduced, and the monitoring process begins once again.

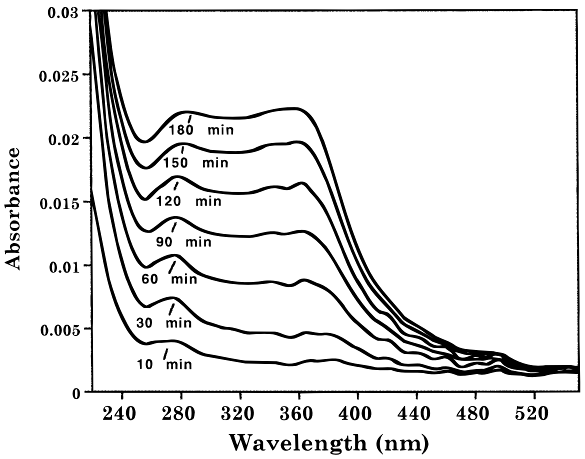

Figure 6. Changes in optical density as a function of time for an aqueous supernatant in contact with a *cis*-$Pt(NH_3)_2Cl_2$-doped hydroxyapatite/porous Si/Si sample. The corresponding time interval associated with a specific spectrum is listed at lower left.

We have also carried out preliminary measurements of the diffusion of *cis*-$Pt(NH_3)_2Cl_2$ from the "doped" apatite/porous Si matrix upon exposure to an aqueous environment (Figure 6). For an as-prepared *cis*-platin-doped apatite/porous Si/Si sample, an increase in the optical density in the 260−400 nm region can be roughly fit to a first-order process, with a corresponding k_{obs} of 2×10^{-3} min^{-1}. However, the species emanating from the apatite matrix into the surrounding medium appears to be an equilibrium mixture of *cis*-platin hydrolysis products, as gauged by the appearance of its characteristic λ_{max} near 280 nm[7] and the absence of the *cis*-$Pt(NH_3)_2Cl_2$ absorption maximum at ~300 nm. An evaluation of the effect of varying the ligand coordination sphere of square planar Pt complexes on the rate of diffusion from a doped apatite/porous Si matrix is currently in progress and the focus of a future publication.

In summary, we have demonstrated that incorporation of

---

[7] Millar, S. E. and House, D. A., *Inorg. Chim. Acta* **1989**, *166*, 189.

stable transition metal complexes within a hydroxyapatite/porous Si/Si matrix can be achieved and that the rate and amount of a complex emanating into the surroundings are controllable.

Note Added in Proof. The use of the term “hydroxyapatite” or “apatite” throughout this paper is not intended to infer a high degree of crystallinity to the as-formed calcium phosphate deposits. Indeed, preliminary structural studies to date suggest that rapid cathodic nucleation (over a time scale of minutes to hours) gives rise to an amorphous phase which under physiological conditions will gradually convert over periods of days to weeks to hydroxy-carbonate apatite (HCA), a defective crystalline form of the material.

Acknowledgment. The authors gratefully thank the Robert A. Welch Foundation and TCU Research Fund for financial support of this research.

Supporting Information Available: A fluorescence micrograph of a $Ru(phen)_3^{2+}$-doped hydroxyapatite/porous Si/Si sample and a plot showing the effect of thermal annealing on the time-dependent changes in the normalized emission intensity of a $Ru(phen)_3^{2+}$-doped hydroxyapatite/porous Si/Si sample upon water exposure (2 pages, print/PDF). See any current masthead page for ordering information and Web access instructions.

JA9823666